EVALUATING URBAN SOLAR POWER POTENTIAL TO ADDRESS TRANSPORT AND RESIDENTIAL ENERGY DEMANDS OF QUEZON CITY, PHILIPPINES

Mathew Harvey T. PERALTA[1] and Yasunori MUROMACHI[2]

[1]Doctoral Student, Dept. of Civil and Environmental Engineering, Tokyo Institute of Technology
(G3-5, 4259 Nagatsuta, Midori-ku, Yokohama 226-8501 Japan)
Asst. Professor, Institute of Civil Engineering, University of the Philippines Diliman
(Pardo de Tavera St., UP Diliman, Quezon City, 1101, Philippines)
E-mail: peralta.m.aa@m.titech.ac.jp (Corresponding Author)
[2]Member of JSCE, Professor, Dept. of Civil and Environmental Engineering, Tokyo Institute of Technology
(G3-5, 4259 Nagatsuta, Midori-ku, Yokohama 226-8501 Japan)
E-mail: muromachi.y.aa@m.titech.ac.jp

The transport and residential sectors command the largest shares of the Philippine energy demand and are currently mostly served by non-renewable sources. To aid in achieving the country's emission reduction targets, there is a need to assess its potential to serve these demands using renewable alternatives. This study aimed to evaluate the solar power potential of its most populous city, Quezon City, calculate the transport and residential energy demands of its residents, and compare the available supply and demand to obtain the necessary generation, charging, storage, and augmentation needs using cost optimization. The residential energy demand of the study area reached 3,691 GWh in 2022, while private car transport, if converted to an all-electric system, would have an energy demand of 946.7 GWh. The estimated annual total incident irradiation in the study area is 1.16 MWh/m^2. The available roof area of 24.5 km^2, estimated using the Segment Anything model and shape analysis, would translate to a theoretical maximum installed capacity of 4.39 GW. However, based on the cost optimization conducted, only a 1.90 GW solar PV installed capacity is needed, together with a 1.75 GWh storage capacity. This will result in an estimated 31% CO2 emission reduction per year. This can be increased with higher solar power generation, though at a higher overall cost. The results of the study can be used to make policy decisions on the use of residential solar panels, vehicle-to-house charging systems, EV adoption, and energy production.

Key Words : *urban scale solar power modeling, transport and residential energy, vehicle-to-home control, cost minimization*

1. INTRODUCTION AND OBJECTIVES

Decarbonizing transport has been identified as one of the most important steps towards averting the climate crisis. One of the strategies involved is the electrification of transport using renewable energy. The goal of this research is to contribute to achieving the GHG emission reduction targets of its study area, the Philippines, by focusing on the use of solar power for its transport and residential energy demands. It aims to show a method for identifying the necessary operation parameters for a solar power and vehicle-to-home system to serve these transport and residential energy demands in an urban-scale analysis.

In 2020, solar power accounted for only 1.2% of the electricity generated and 0.2% of the total energy used in the Philippines. With transport and residential energy demands comprising 30.4% and 31.0%, respectively, of the energy demands of the country, the conversion to solar power would greatly reduce its GHG emissions[Note 1)]. The hourly potential for solar power of the country has not yet been clearly studied, specifically in relation to urban environments where space is limited for solar power generation. Multiple studies have shown how to implement solar PV generation (and its related costs) in combination with energy storage systems in addressing residential energy demand[1–4)]. However, for the case of transportation energy, studies on the integration of solar power are scarcer since most studies employ aggregated energy calculations[5–7)]. The hourly demand would be needed to identify the times at which the vehicles are in use and those at which they are parked and available for charging. This would be essential to be able to compare the total residential and transport demands with the available supply, which would then allow for the calculation of the augmentation and storage requirements Existing studies have tried assessing the use of solar power for the combined residential and transport energy demand, though only ranging from one household[8–10)] to 148 households/apartments[11)], but seldom in a city scale.

This study focused on investigating the solar

power potential of an urban area, calculating the energy demands from the transport and residential sectors, and comparing the available supply to the demand to obtain the necessary generation and charging patterns and assess the need for storage and augmentation using cost minimization. The rest of the paper is structured as follows: section 2 discusses studies on the application of V2H systems in serving energy demands of different cities, as well as its integration with renewable energy sources; section 3 describes the study area and related energy statistics; section 4 outlines the methods used in the 4 main parts of the study: residential energy demand calculation, transport energy demand estimation, solar power modeling, and cost optimization for the supply-demand operating parameters; section 5 discusses the pertinent results; and finally, section 6 lists the relevant conclusions.

2. VEHICLE-TO-HOME (V2H) SYSTEM

Vehicle-to-home (V2H) and vehicle-to-building (V2B) technology, which allows two-way energy transfer between EVs and buildings/houses, is seen to lead to higher EV shares since it converts EVs into "rolling storage" for the grid providing both flexibility and mobility. Different studies have explored different aspects of the integration of V2H systems in serving energy demands such as charging patterns, travel schedules, EV mix, and seasonal differences. It has been shown in a study in Denmark that the charging patterns in public stations are starkly different from that of households. Public station charging peaks around midday, presumably because of more outside activities around that time. Private, or residential charging, mostly starts around 5-6PM and increases until midnight and decreases thereafter[12]. Another study on EV integration in Greece showed that about 75% of charging sessions are home charges, specifically regular night charges (53.3%) and residual charges (22.1%). Home charges usually start at night/late afternoon, whereas work and residual charges are done midday. Interestingly, fast charging is seen all throughout the day. The study also presented distribution differences between days of the week. The overall load for a weekend is lower than a typical weekday, and the charging pattern, especially for the start times of fast charging and residual charging are slightly different[13].

V2H has also been seen as beneficial in improving renewable energy (RE) integration since it provides the storage needed to alleviate the problems with limited generation time associated with REs such as solar and wind power[14,15] A system involving solar PV, EV, V2H, and stationary storage have been shown to be more economical in households wherein EVs are in use (for driving) longer, and hence are less available for charging/discharging. This system also improved the self-sufficiency and energy-saving rates of households[16]. V2H has also been shown to improve the solar PV self-consumption rate by shifting the surplus energy from the peak generation times to the peak consumption times as well, and reduce the dependence on the grid, even during peak hours[10].

In terms of cost, it has been shown that if charging/discharging is controlled, EVs actually mostly charges during the daytime where there is solar PV generation, and discharges at night to serve the household demand[17]. This is in contrast with typical assumptions in most studies where EVs are usually charged at night. This is an interesting point that was also observed in the current study.

As for the costs considered in implementing the system, the studies reviewed included the following variables: cost of acquiring electricity from the grid, installation and operating/maintenance costs of the solar PV, V2H, and storage systems, selling price of electricity to the grid, subsidies for solar PV generated electricity, and EV acquisition and operating costs. Aside from cost, other studies have optimized the solar PV-V2H-stationary storage systems using other objective variables such as power loss[15] and CO_2 emissions[18].

Currently, most studies on EV and V2H integration, and its effect on transportation and residential energy consumption are understandably focused on European cities with a fairly high EV penetration, whereas studies on Southeast Asian cities, let alone on Philippine cities, are limited.

3. STUDY AREA



Fig. 1 *(L)* the Philippines; *(R)* Quezon City

The area considered in this research was Quezon City (QC), Philippines. It was the capital of the Philippines from 1949-1976 and is the largest city in the

National Capital Region (NCR), also known as Metropolitan Manila. It has an official area of 16,112 hectares, or about a quarter of the land area of NCR. As of 2018, residential areas, including socialized housing and informal settlement, comprise about 32% of the city, or about 5,100 hectares. It also includes a significant amount of institutional areas since it previously served as the nation's capital[Note 2)]. Based on the 2020 census, the city has a population of 2.96 million, or about 22% of the population of NCR and 2.7% of the whole country[Note 3)].

Private cars dominate daily traffic in the city with about 38% of the average daily passenger volume. Public transport modes consisting of jeepneys, buses, taxis, UV, and tricycles comprise about 55%, and private motorcycles serve the remaining 7%[Note 2)]. In terms of transport energy, there is no specific data for the city only. However, country estimates shows that fossil fuels (gasoline and diesel) serve 95% of the demand, while less than 0.1% uses electricity[Note 1)].

As for the electricity in QC, it is connected to the Luzon Grid that had a total installed capacity of 19.7 GW and a total generated power of 79,820.5 GWh in 2022. This grid power generation is actually more dependent on fossil fuels (coal, oil, and natural gas) at 85% compared to the global total at 63%. The solar power generation share is also less than the installed capacity share, presumably because of the limited time that solar power plants can operate compared to fossil fuel-based ones which can operate at any given time in most weather conditions. Among the total energy consumed of 80,868.3 GWh in the grid, the residential sector consumes the most at 32%, followed by the commercial (26%) and industrial (24%) sectors. With the high dependency of the power generation on coal, of which 60% is imported, the residential energy supply would greatly benefit from a clean and indigenous source like solar power.

In terms of CO_2 emissions, Filipinos emitted 1.2 metric tons per capita in 2020. This is significantly lower than the world average of 4.3 and those from its southeast Asian neighbors in Indonesia (2.1), Thailand (3.7), and Malaysia (7.4) [Note 4)]. However, from energy use alone, it is estimated that Filipinos emit 1.09 tCO_2e per capita[Note 1)], which is 90% already of the total per capita emissions. Hence, they would benefit greatly from the reduction in emissions resulting from the conversion to solar power.

4. METHODOLOGY

(1) Residential Energy Demand

The residential energy demand data were from the Department of Energy (DOE) and National Grid Corporation of the Philippines (NGCP) statistics. These included the monthly electricity consumption per region and hourly demand per grid[Note 5)], and monthly electricity consumption per grid by sector[Note 6)] for the year 2022.

What is needed is the hourly residential energy demand of QC residents. However, the only available hourly data is on a grid level (QC belongs to NCR which is connected to the Luzon Grid). The percentage of residential energy demand for the Luzon Grid is available on a monthly rate only, hence the monthly percentage was assumed to apply. Similarly, the percentage of energy consumed by NCR residents for the Luzon Grid is also available. Lastly, to get the QC residential energy demand, specifically, the ratio of the population of QC to that of NCR (21.95%) was used. An argument could be made that the ratio of the number of households be used instead of the population. However, the statistics from the 2020 census showed that households in QC made up 21.11% of the total households in NCR, hence the difference would have been negligible.

(2) Transport Energy Demand

The traffic data was mostly sourced from the MMUTIS Update and Enhancement Project (MUCEP) database. This database is based on the results of vehicle counts and household information surveys done in Metro Manila and adjacent areas from 2013-2014[19)]. The main data used from this project were the household trip results detailing typical weekday trip history of each household member interviewed. The details include the departure and arrival times, origin-destination, and mode used. Hence, the car trips used by residents of Quezon City could be isolated. To be able to project to the current demand, the number of cars registered from the Land Transportation Office (LTO) was used. The data showed that the total number of private cars in NCR grew by 9% from 2020 to 2021. Hence, for 2022, a total number of cars in NCR is estimated to be 850,000, or 187,000 in Quezon City. For the variation between typical weekdays and weekends, ratios from traffic counts of the Department of Public Works and Highways (DPWH) were used. These allowed the estimation of trips and corresponding transport energy demand to be varied between weekdays and weekends/holidays since the MUCEP database only captured typical weekday trips.

Only trips from QC residents were considered. For trips that involved multiple modes (e.g., drive to train station, park, then take train to work), only the leg using the car was considered. The total vehicle-kilometers traveled per hour of all car trips surveyed

were tabulated and projected to 2022 values by multiplying the ratio of currently registered vehicles in QC to the number of cars surveyed.

For the energy demand in terms of tonnes of oil equivalent (toe), a fuel efficiency value of 5.59 km/L[20] was used. The values in liters were then converted to thousand barrels of oil (1 thousand barrel of oil = 158987 L). The calorific value used to convert from thousand barrels of oil to toe was 1223 toe/thousand barrel of oil[Note 1].

The energy demand when converted to EVs would be in kWh. Hence the hourly VKTs were converted using the consumption rate of the EV selected. The EV used in this study has an equivalent consumption rate of 6.9 kWh/km.

(3) Solar Power Modeling

The irradiance modeling performed follows the steps discussed in [21,22] with the following major steps: solar positioning, global irradiance decomposition, and plane of array irradiance calculation.

The main input data were the meteorological data, current solar panel specifications, and Google Earth Satellite images (GSI) of the study area. Meteorological data including temperature and solar radiation were obtained from the Philippine Atmospheric, Geophysical and Astronomical Services Administration (PAG-ASA) for 2022. Based on a Voronoi analysis of the location of existing weather stations, station 98, or the Science Garden automatic weather station (latitude 14.664778; longitude 121.001807) was determined to cover the study area. Since the available data varied from 10min to 1 hr values, they were averaged per hour for the study period. The solar panel specifications used are shown in Table 1.

Table 1 Solar Panel Specifications

Solar Panel Parameter	Value
Rated Maximum Power [W]	400
Temperature Coefficient [%/ºC]	-0.35
Area [m^2]	2.015X0.996m = 2.00694
Module efficiency [%]	19.9
Tilt [º]	30
Azimuth [º]	0

For the rooftop images, though orthophotos were obtained from the National Mapping and Resource Information Authority (NAMRIA) of the Philippines, the quality was deemed not usable for the purposes of this study due to the zoom level at which they were taken, making the boundaries between buildings unclear. Hence, this study used openly available Google Earth Satellite images (GSI) for the study area.

The actual modeling was implemented through MATLAB. After the solar positioning calculations based on the latitude and longitude of the weather station, the components of solar radiation on a horizontal surface, Global Horizontal Irradiance, *GHI*,, were calculated. These components are the Direct Normal Irradiance, *DNI*, and Diffuse Horizontal Irradiance, *DHI*. The relationship between these components, based on the zenith angle, *z*, is given by:

$$\boldsymbol{GHI = DNI}\cos \boldsymbol{z + DNI} \qquad (1)$$

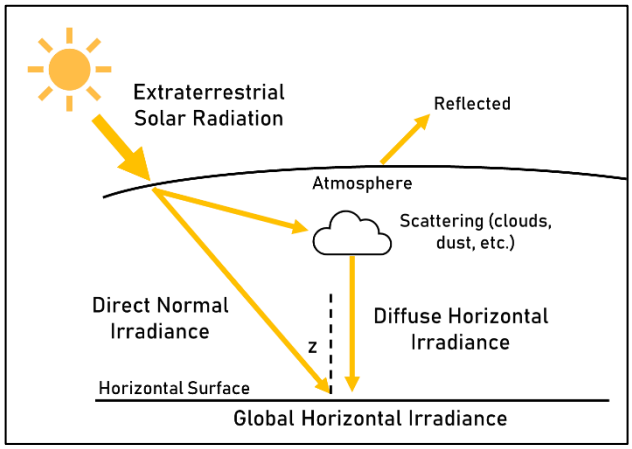


Fig. 2 GHI Components

Given that *GHI* is measured on site, the clearness index, k_t, defined as the portion of the extraterrestrial radiance received on a horizontal surface on Earth, I_{ES}, was calculated as

$$\boldsymbol{k_t = \frac{GHI}{I_{ES}}} \qquad (2)$$

When *GHI* is measured on-site, it is only imperative to calculate one of the components independently since the other can readily be obtained based on Eq (1). The ratio, k_d, of the diffuse component, *DHI*, to the *GHI* used on this study followed the Erbs model[23], since hourly data was similarly utilized in this model instead of the commonly used monthly averages in other studies.

$$\boldsymbol{k_d = \frac{DHI}{GHI}} \qquad (3)$$

Once these components were determined, the irradiance on a tilted surface (e.g., solar panel) were obtained. There are three components: the Beam/Direct Irradiance, I_b, the Diffuse Irradiance, I_d, and the Reflected Irradiance, I_r. The beam component, I_b, was directly obtained from the geometric conditions based on the position of the sun at any time (incidence angle, *i*). The reflected component, I_r, is based on the panel tilt, β, and albedo, or the reflectance of

the surface. For ordinary ground or grass, the albedo is taken to be 0.2 [21]. Lastly, the diffuse component, I_d, was calculated based on the factor, f_d, calculated from the Perez anisotropic model[24].

$$I_b = DNI \cos i \tag{4}$$

$$I_r = GHI \frac{0.2(1 - \cos \beta)}{2} \tag{5}$$

$$I_d = DHI(f_d) \tag{6}$$

$$I_T \left[\frac{Wh}{m^2}\right] = I_b + I_r + I_d \tag{7}$$

The total incident irradiance on a tilted surface was obtained using Eq (7). This was then converted into actual solar power based on the solar panel specifications and the available area for generation (installed capacity). Adjustment factors for temperature effects (0.95) and shading and dust (0.80).

A combination of the Segment Anything Model (SAM)[25] and shape analysis was used to estimate the total available roof area for solar power generation in the study area. Specifically, this study utilized the segment-geospatial (samgeo) package which allows the use of SAM for geospatial data analysis with minimal coding[26]. It was implemented through Google Colab, looping through GSIs until the whole study area was covered. A sample result of the generated masks from a satellite image is shown below.

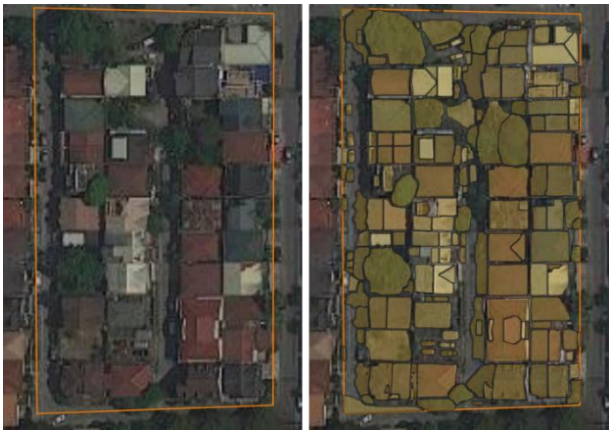


Fig. 3 Sample Image Segmentation Results:
(L) Google Earth Satellite Image;
(R) Masks Generated with SAM/samgeo

The next phase was the use of shape indices to remove (most of) the non-building features. The first step was to apply the "Simplify" tool to the features since they were converted from a raster to a vector causing them to have saw-like edges representing pixels. The tool would smoothen out the edges of the features. Then, filtering using shape indices was done. Features with areas larger than 3000 m^2 were removed since buildings rarely have an area of this size and these features usually represent background (open lots, water features, etc.). Those with areas smaller than 25 m^2 were also removed not only because cars and small trees usually fall under this category, but also because roofs of this size would be too small for solar power applications. Aside from the shape area, three main indices were used in this study: circularity, circularity of the convex hull, and the effective rectangularity index[27]. Initially, circularity is used to remove most trees since they tend to be more circular than buildings. However, it was observed that some trees (or adjacent trees) form a more oblong or even U-shaped clusters, hence it was decided to use the convex hull of the shapes which represents the minimum convex polygon that encloses all the points in the shape. A sample is shown in Figure 4 where the feature shown is for a group of trees segmented into one feature. To illustrate, the circularity of the segmented feature shown is 0.293, while the circularity of its convex hull (CCH) is 0.803. In comparison, a square feature would have a circularity of 0.785 while rectangles would have an even smaller value. Hence a threshold of 0.8 was used for the circularity of the convex hull. The problem with the use of this index alone would be U-shaped and L-shaped structures would also have a high value since their corresponding convex hulls would be more rounded. Hence, the effective rectangular index (ERI) was also employed in identifying tree-like features. This index aims to improve the problem with the more commonly used "rectangularity index" which is too sensitive to overhangs / protrusions in mostly rectangular shapes. ERI is the ratio of the perimeters of the equal-area rectangle of a shape to that of the shape itself[27]. It has a value of 1 for perfect rectangles and 1.128 for circles. Generally, rounded shapes have an ERI greater than 1. For the cases of U-shaped and L-shaped structures, ERI was found to be lower than 0.8. Hence, to remove most tree-like features, those with both CCH and ERI >0.8 were filtered out.



Fig. 4 Sample Shape Index Illustration

CCH was also used to remove long and thin features such as roads and river sections since these shapes were found to have circularities less than 0.2. Lastly, complex shapes with a significant number of edges and/or vertices needed to be removed since

they represent objects like the outline of closely spaced row houses and open fields with multiple holes. Features like these were found to have ERI values less than 0.3. To summarize, the criteria used to filter out the features are shown in Table 2.

After application of these indices, manual cleaning was also implemented to remove remaining obvious non-buildings such as trees, roads, and river sections to improve the accuracy of the estimate. The total areas of the remaining features were then summed up and used in the calculation of the maximum solar power generation capacity.

Table 2 Shape Analysis Criteria for Removing Features

Criteria	Target Features
Area > 3000 m^2	Background and open lots
Area < 25 m^2	Cars and small trees
CCH > 0.8 and ERI >0.8	Round objects like trees
CCH < 0.2	Long thin objects like roads and building gaps
ERI < 0.3	Outline of closely spaced buildings

(4) Cost Minimization

In order to actually determine the hourly transport energy demand, the amount of energy demand from charging the vehicles per hour must be obtained. This is usually dependent on the user preference and availability. Previous studies have used a probability distribution obtained from surveying current users. However, since EV usage in the Philippines is not yet prevalent, this approach is not feasible. Another method used is charging control based on cost minimization[18,28]. Basically, the assumption is that provided that the residential energy demand and the transport demand for the next trip is met per hour, and the totals per day and per year, the time at which charging (and possibly discharging), and its duration can be controlled to come up with the lowest cost.

Hence, in this study, cost optimization (minimization) was conducted to determine the appropriate charging and discharging times of the EVs and the stationary storage (referred to as BAT from here),. For simplification, each EV's condition was checked per hour (in use or parked) and it was assumed that if parked, then it was available for charging regardless whether it was at home or at a different location. The stationary storage was also assumed to be one giant storage capable of charging/discharging to any household in the study area. It was also assumed that both the buying and selling prices of electricity from and to the grid are constant. The cost of buying all the EVs was not considered since it was assumed that conversion to EV will happen regardless of the implementation of the solar PV – V2H system.

The input parameters are summarized in Table 3. The independent variables considered in the optimization were the required solar PV capacity, ***capPV***, amount of electricity bought per hour, $\boldsymbol{pw_{buy,t}}$, EV charge/discharge per hour, $\boldsymbol{load_{EV,t}}$, and stationary storage charge/discharge per hour, $\boldsymbol{load_{BAT,t}}$. The required storage capacity, ***capBAT***, was also varied, but discretely, per run to determine the setting leading to the least cost.

Table 3 Optimization Parameters Considered

Parameter		Unit	Symbol	Value*
Electricity Pricing				
	Buying price	PhP/ kWh	pr_{buy}	10.4 (0.19)
	Selling price	PhP/ kWh	pr_{sell}	3.6 (0.065)
PV Cost Parameters				
	Installation cost	PhP/kW	ic_{PV}	100,000 (1,818.2)
	Operating cost	PhP/ kW/yr	oc_{PV}	1,250 (22.7)
BAT Parameters				
	Installation cost	PhP/ kWh	ic_{BAT}	19,910 (362.0)
	Operating cost	PhP/ kWh/yr	oc_{BAT}	0.0165 (0.0003)
PV Operating Parameters				
	Maximum PV installed capacity	kW	$capPV_{max}$	**
EV Operating Parameters				
	Total EV capacity	kW	capEV	7,480,000
	Charging rate	kW	EV_{ch}	3
	Discharging rate	kW	EV_{dis}	-6
	Initial charge	%	-	90
	EV fuel economy	km/kWh	-	6
	Charging/discharging efficiency	-	eff_{EV}	0.8
BAT Operating Parameters				
	Storage Capacity	kWh	capBAT	***
	Charging rate	kW	BAT_{ch}	0.5
	Discharging rate	kW	BAT_{dis}	-0.5
	Initial charge	%	-	50
	Charging/discharging efficiency	-	eff_{BAT}	0.8

*values in ( ) are in USD when applicable @ 1USD = 55 PHP
**dependent on total available roof area
*** values set discretely to keep objective function linear

The main objective function considered (similar to [18]) was:

(8)

$$\min Total\ Cost\ = IC + \sum_{y=1}^{25} \frac{OC + C_{buy} - I_{sell}}{(1+r)^{y-1}}$$

where
IC = initial cost = $icPV \times capPV + icBAT \times capBAT$
OC = operating cost = $ocPV \times capPV + ocBAT \times capBAT$
C_{buy} = cost of bought electricity = $prbuy \sum_{t=1}^{365*24} pwbuy_t$
I_{sell} = income from selling electricity
$= prsell \sum_{t=1}^{365*24} (E_t capPV + pwbuy_t - loadEV_t - loadBAT_t - D_t)$
r = social rate of return = 10%[Note 7)]
y = considered life span of system=25 years
E_t = incident irradiance at hour t per kW installed
D_t = residential energy demand at hour t

It was subjected to the following constraints:

- Limits on installed solar power capacity:

$$0 \le \boldsymbol{capPV} \le capPV_max \quad (9)$$

- Limits to EV charging and discharging:

$$\sum_{i=1}^{N_{EV}} (EV_{dis} \times cond_{i,t}) \le \boldsymbol{load_{EV,t}} \le \sum_{i=1}^{N_{EV}} (EV_{ch} \times cond_{i,t}) \quad (10)$$

where $cond_{i,t} = 0\ if\ in\ use; 1\ if\ parked$
$N_{EV} = number\ of\ EVs$

- Limits to BAT charging and discharging:

$$BAT_{dis} capBAT \le \boldsymbol{load_{BAT,t}} \le BAT_{ch} capBAT \quad (11)$$

- Minimum total EV charge up to hour t:

$$\left(\sum_{i=1}^{N_{EV}} \sum_{k=1}^{t} const_{i,k} \right) - 0.9 capEV \le \sum_{k=1}^{t} load_{EV,k} \times eff_{EV} \quad (12)$$

where $const_{i,k}$ = energy consumed by EV i at hour k

- Maximum total EV charge up to hour t:

$$\sum_{k=1}^{t} load_{EV,k} \times eff_{EV} \le \left(\sum_{i=1}^{N_{EV}} \sum_{k=1}^{t} const_{i,k} \right) + (1 - 0.9) capEV \quad (13)$$

- Limits to total BAT charge up to hour t:

$$-0.5 capBAT \le \sum_{k=1}^{t} load_{BAT,k} \times eff_{BAT} \le 0.5 capBAT \quad (14)$$

- End of year return to initial EV charge:

$$\sum_{t=1}^{365*24} \boldsymbol{load_{EV,t}} \times eff_{EV} = \sum_{i=1}^{N_{EV}} \sum_{t=1}^{365*24} const_{i,t} \quad (15)$$

- End of year return to initial BAT charge:

$$\sum_{t=1}^{365*24} \boldsymbol{load_{BAT,t}} \times eff_{BAT} = 0 \quad (16)$$

- Supply-demand balance:

$$E_t \boldsymbol{capPV} + \boldsymbol{pw_{buy,t}} - (\boldsymbol{load_{EV,t}} + \boldsymbol{load_{BAT,t}} + D_t) \ge 0 \quad (17)$$

Since the purpose of the study was to maximize the use of solar power in addressing the transport and energy demands, the amount of electricity that could be bought from the grid was limited to the current residential demand per hour.

As mentioned earlier, *capBAT* was varied discretely instead of included in the variables to be adjusted in optimization. The *capBAT* value with the lowest corresponding total cost was considered the optimal setting. The optimization was done through the *linprog* module of MATLAB.

5. RESULTS AND DISCUSSION

(1) Residential Energy Demand Profile

Based on the estimates for Quezon City, the 2022 total residential energy demand reached 3,691 GWh. This means that for the estimated 2022 population of the city of 3.121 million, the per capita residential electricity demand is 1.2 MWh/person per year. This is 33% higher than the country average of about 0.9 MWh/person.

The average hourly demand per season is shown in Figure 5 while that comparing weekend and weekday averages is shown in Figure 6. Demand is lowest ataround 3-6AM and highest at around 11AM-2PM. This is mostly due to difference in cooling requirements in households. The annual hourly average ranges from 350-480 MWh. The weekday demand is also consistently higher than in the weekends, though the demands from midnight to 4AM are similar. The average hourly weekday demand peaks at 496 MWh while the weekend demand peaks at 424 MWh, both happening from 12NN-1PM. Though averages are shown here for discussion purposes, the actual hourly

measurements were used in the optimization.

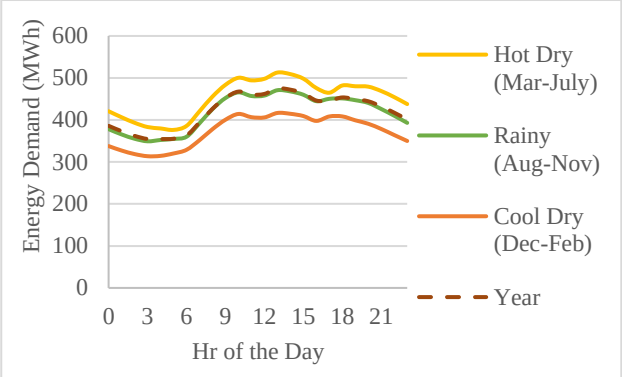


Fig. 5 Ave Hourly Res. Demand: Seasonal Variation

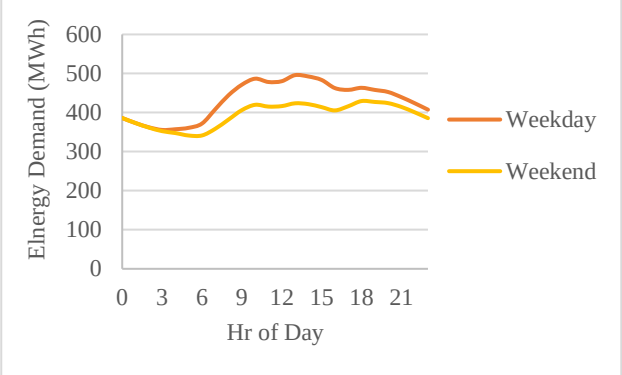


Fig. 6 Ave Hourly Res. Demand: Weekday vs Weekend

(2) Transport Energy Demand Profile

As mentioned before, the total number pf private cars registered in QC in 2022 is about 187,000. Based on the results of the MUCEP household survey, the number of private cars in use for QC residents peaks to about 88,000, or 47% of the total, at around 6-8AM presumably for travel to work and schools. This volume stabilizes at around 20,000-40,000 cars during midday before increasing again to about 50,000 at around 5-7PM. For the typical weekend volume, the ratios of average hourly weekday to weekend traffic from DPWH traffic counts were used. Based on this estimate, the period of the morning and afternoon peaks are similar to that of the weekday, though the volumes are different. The morning peak is lower than that during weekdays (only 31% of the total, compared to 47% during weekdays), indicative of more people tending to wake up later during weekends. On the other hand, the afternoon peak is higher by about 20% signifying more activities (and consequently, more trips) done at later hours of the day.

(3) Solar Power Generation

Based on the GHI measurements from the weather stations, the total irradiance per hour were calculated using the method discussed earlier. The hours in between sunrise and sunset (solar hours) in the Philippines do not vary significantly throughout the year, hence irradiance is only observed from 6AM-7PM. Peak irradiance happens around 11AM-1PM, ranging from 400-500 Wh/m^2. The average daily total differs from the estimates of the Global Solar Atlas[Note 8)] using the same panel tilt and azimuth by 0.4% (January) to 24% (August). Variation is expected since the Solar Atlas uses long-term yearly averages while the calculation made in this study is for 2022 only. The total annual irradiance calculated is 1.16 MWh/m^2.

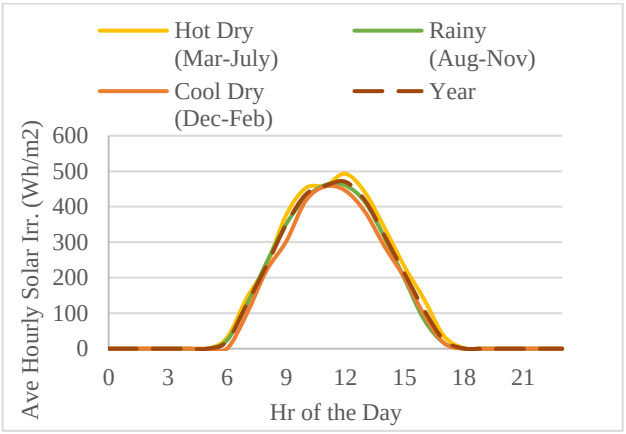


Fig. 7 Ave Hourly Total Irradiance: Seasonal Variation

In terms of seasonal variation, the traditionally sunny periods from March to July in the Philippines have slightly higher average hourly irradiances, though their monthly totals are significantly higher, especially March and May. Interestingly, rainy periods from August to November have higher average hourly values compared to dry months from December to February. This signifies that even though this period experiences more rainy days, the latter period experiences more cloudy days.

After subjecting the total area of the study area (161 km^2), a total of about 280,000 features were left. This does not correspond to the actual number of buildings in the study area since some roofs were segmented into different features due to boundaries between some roof sections. Figure 8 shows a sample of the resulting features after the segmentation and shape analysis conducted. Though the method visually worked well for low to medium density structures since the effect of height does not affect the footprint significantly, it had trouble with high-rise structures such as condominiums. This was also observed in [29] since they also used Google Satellite images which were not orthorectified. Hence, for these areas, manual cleaning was needed to remove walls and windows since their shapes are mostly rectangular, closely resembling roofs, and hence were not filtered out by the shape indices used.

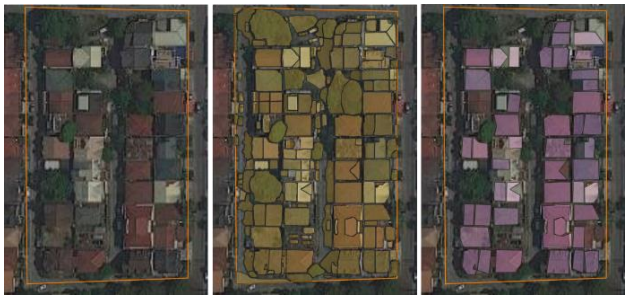


Fig. 8 Sample Result of Segmentation and Shape Analysis: *(L)* Satellite Image; *(C)* After Segmentation; *(R)* After Shape Analysis and Cleaning

The method consistently underestimated the total area available in the sections used for validation. This is mostly because of irregularly shaped roof areas. As mentioned before, the shape analysis aims to determine mostly rectangular and triangular features, which is true for most structures. However, because of shading from trees, visible portions of some roofs become more rounded, and hence are more likely to be filtered out by the indices used. This is an inevitable limitation of the indices and images used. Medium/high-rise structures were labeled as false negatives (in comparing actual to segmented features) since the resulting shapes of the roofs of these structures are mostly irregular due to the presence of competing uses placed on these structures such as vents and tanks. This is another area where the method appears to be limited as shown in lower *Recall* values. That said, the *Precision* of the method is consistently high (73-88%), signifying that when the model identifies a feature as a building roof, the probability that it is indeed a building roof is high. It shows that the method works for clearly delineated features without much obstruction from trees and shadows from taller structures. The underestimation of actual available roof areas for solar power generation provides a conservative estimate than the actual total area available.

The total available roof area estimated through the segmentation and shape analysis conducted is 24.5 km^2 in the whole city. As mentioned earlier, the annual total residential energy demand in QC is 3,691 GWh, while the annual transport energy demand is 946.7 GWh, for a total demand of 4,637.7 GWh. The total annual irradiance calculated was 1.16 MWh/m^2. Using an 80% reduction factor to account for shading and other environmental factors, and a 95% factor for ambient temperature effects, for the solar panel specifications used, the demand would require about 26.3 km^2 of solar power generating area. These parameters would translate to 4.39 GW of maximum installed capacity, *capPVmax*. Hence, theoretically, the available area can almost cover the entire demand. However, due to the time dependence of solar power generation, residential demand, and vehicle availability for charging, it is important to assess the temporal component to check the viability of the system. The roof area estimated would only serve as an upper limit to the solar power that can be generated.

(4) Cost Minimization

The independent variables considered were the required solar PV capacity, amount of electricity bought per hour, EV charge/discharge per hour, and storage charge/discharge per hour. The required storage capacity was also varied, but discretely, per run to determine the setting leading to the least cost.

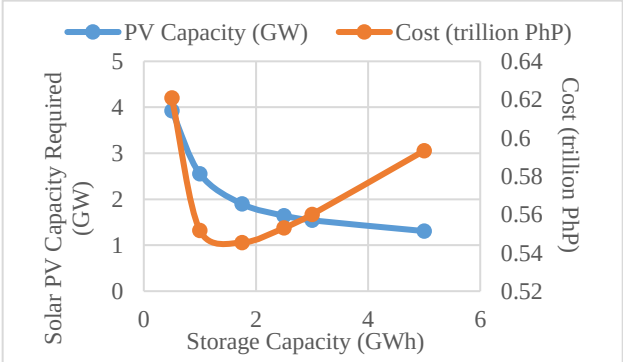


Fig. 9 Cost Minimization Results for Varying Stationary Storage Capacities

Figure 9 shows the variation of the required PV capacity and resulting cost at different storage capacity levels. The PV capacity needed decreased as the storage capacity increased. Low storage capacity results in more buying from the grid and a higher solar PV capacity requirement since there are no other sources to serve the demand, especially during peaks. High levels of storage reduce the need for solar PV generation since there is a higher volume available at most times. The lowest cost of about PhP 0.55 trillion (USD 10 billion) is attained at 1.75 GWh storage capacity with a 1.90 GW solar PV capacity.

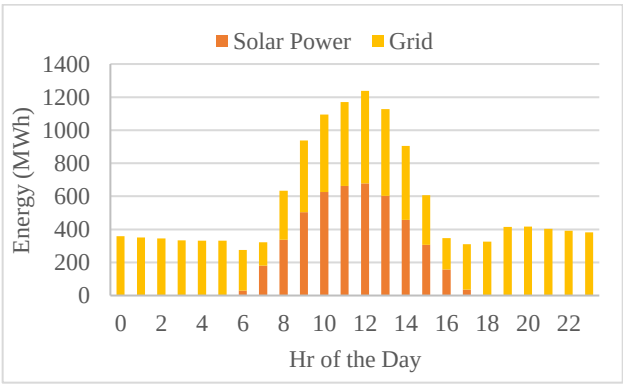


Fig. 10 Ave Hourly Energy Production

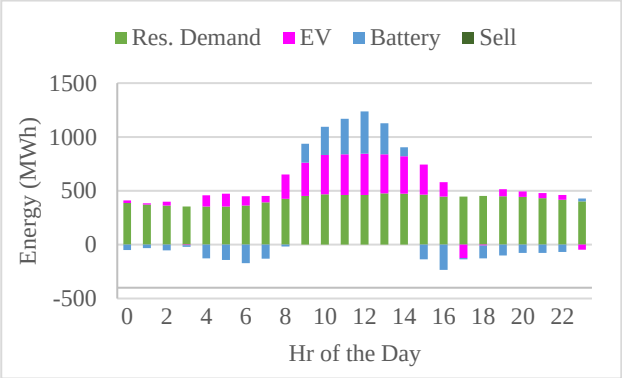


Fig. 11 Ave Hourly Energy Demand

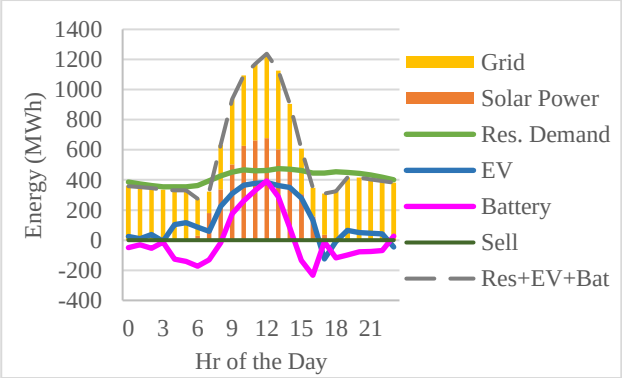


Fig. 12 Average Hourly Energy Supply and Demand

Figures 10-12 show the resulting supply and demand pattern from the least cost operating parameters. During non-solar hours, energy demand is served from energy bought from the grid and stationary storage. EVs and the storage are charged mostly during midday when solar power generation is abundant. EV discharge is rarely used to serve the residential demand. This is presumably because the solar power generated only exceeds the residential demand during 11AM-2PM, hence not much surplus is obtained. Since that surplus is not very high, there is less energy to distribute during the non-solar hours. There is also a distinct discharging period from the EVs at around 4-6PM because the residential demand, D_t, is still high but there is low solar power generation. Minimal selling is observed since the price is low. Hence, demand is the biggest factor in determining the required solar PV capacity, instead of income from selling surplus energy. Theoretically, the amount of selling could be increased if the solar power capacity is increased given that there is more available based on the roof area. However, this would increase the installation and operating costs of PV.

(5) CO_2 Emission Reduction

To understand the impact of the shift in terms of CO_2 reduction, the annual emission levels for two scenarios were considered: (1) Business as usual (BAU); and (2) With solar PV-V2H-BAT system. For the energy bought from the grid, the carbon intensity of the current Philippine energy mix was obtained from Ember's yearly electricity data[Note 9)]. For 2022, the Philippine energy mix was estimated to emit 582 gCO2e/kWh. As for the current transport energy demand, gasoline-fuel vehicles have an emission factor of 506 gCO2e/km while diesel-fuel ones emit 319 gCO2e/km[5]. Lastly, it has been estimated that life-cycle emissions for energy generated using solar power to be less than 50 gCO2e/kWh[Note 10)]. Hence, based on the data above, the use of the solar PV-V2H-BAT system with the least cost (storage capacity of 1.75 GWh) would reduce the CO_2 emissions of the study area from 2.84 to 1.95 MtCO2e per year, or a 31% reduction. Though this figure is an already significant reduction, this can be increased by using a higher solar power installed capacity. This will inevitably lead to higher costs, especially considering the relatively low selling price of electricity to the grid compared to the buying price. This shows the need to identify the priority in terms of optimization due to the competing interests of cost minimization and CO_2 emission reduction. That said, as the price of electricity from the gird increases and the installation and operating costs of solar power systems decreases, the benefits of the system proposed is seen to increase in the long run.

Table 4 CO_2 Emission per Scenario

Energy Demand/ Supply	**Activity per Scenario**		**CO_2 Emission Rate**	Emission per Scenario **(MtCO2e = 10^{12} gCO2e)**	
	BAU	PV-V2H-BAT	(10^6) gCO2e/ unit	BAU	PV-V2H-BAT
Energy from grid (GWh)	3,691	3,203	582	2.15	1.86
Vehicle-km using gasoline (10^6 km)	1,135	0	506	0.57	-
Vehicle-km using diesel (10^6 km)	360	0	319	0.11	-
Energy from solar PV (GWh)	0	1,671	50	-	0.08
			Total	**2.84**	**1.95**

6. CONCLUSIONS AND FUTURE STUDIES

The main goal of this research was to contribute to the reduction of GHG emissions by focusing on the use of solar power for addressing transport and residential energy demands. This is important in the context of the study area wherein current residential and transport energy demands are served predominantly through imported, high emission fossil fuel-based sources. The annual residential energy demand reached 3,691 GWh as of 2022, or 1.2 MWh per person per year. As for the transport energy demand, based on the results of the MUCEP study in 2014, the hourly demand was estimated based on typical weekday travel. The peak usage of private cars happens at around 6-8AM to 47% of the total cars registered. This volume stabilizes at around 20,000-40,000 cars during midday before increasing again to about 50,000 at around 5-7PM. This translates to an annual demand of about 350 ktoe. For the case of implementation of the solar PV-V2H-BAT system wherein all the vehicles are converted to EVs, this would translate to an additional electricity demand of 946.7 GWh for the year. Hence, with this level of demand, a shift would greatly benefit the study area. This is also supported by the solar power potential of the study area. The results showed that the total annual irradiance is 1.16 MWh/m^2 in the study area. Hence based on the solar panel specifications discussed, the total demand could be served by solar power alone with about 26.3 km^2 of solar power generating area. An estimated 24.5 km^2 of roof area is available for solar power generation. However, due to the temporal variability of both the supply and demand sides considered, especially in the case of solar power and transport energy demand, as well as consideration of cost, optimization was done to determine the required solar power generation installed capacity, storage capacity, and augmentation from the grid. The results showed that a stationary storage capacity of 1.75 GWh would lead to the least cost for the system inputs considered. This requires a solar power generation installed capacity of 1.90 GW, or only 43% of the maximum available value. Lastly, a 31% reduction in CO_2 emissions is estimated if the proposed system is implemented.

For future studies, the transport energy demand estimate could be improved by using actual trip diaries or machine learning methods. Studies on this variation would also improve the estimate of available cars for charging/discharging. Varying levels of EV integration would also improve the quality of the results since the sensitivity to this would be revealed.

As for the solar power generation, models developed from remotely sensed data relating to other meteorological parameters such as cloud cover, air quality, and suspended particles, as well as time history data could also be looked into. Different roof estimation methods could also be compared, especially 3D city models and machine learning applications that would allow the identification of actual roof slopes and azimuths. Competing usages such as vents and tanks could also be surveyed to further improve the estimate.

Lastly, different scenarios and settings could be investigated in the cost optimization. For example, the case where the amount of electricity augmented from the grid is limited to the deficit from the maximum solar power generating capacity can be considered as the minimum augmented amount needed. Different pricing structures would be interesting to determine the levels at which selling back to the grid becomes viable, especially considering government subsidies and cost reductions due to technology development.

ACKNOWLEDGEMENTS: The authors would like to acknowledge multiple agencies that provided data for this study including PAG-ASA, Department of Energy (DOE), Department of Transportation (DoTr), and the National Center for Transportation Studies (NCTS). We would also like to acknowledge the Japanese Government Ministry of Education, Culture, Sports, Science and Technology (MEXT) for the scholarship it provided.

NOTES

Note 1) Department of Energy. *2020 Key Energy Statistics*. 2020.
Note 2) Quezon City LGU. *Quezon City 2018 Ecological Profile*. Quezon City, Philippines, 2020.
Note 3) PSA. *2020 Census of Population and Housing*. 2021.
Note 4) The World Bank. CO2 Emissions (Metric Tons per Capita). *Climate Watch Historical GHG Emissions* (1990-2020). climatewatchda-ta.org/ghg-emissions.
Note 5) NGCP. *Operations Data*. https://www.ngcp.ph/operations#operations.
Note 6) Department of Energy. *2022 Philippine Power Statistics.* https://www.doe.gov.ph/energy-statistics/philippine-power-statistics.
Note 7) DOF, and NEDA. *Memorandum Re: Updated Social Discount Rate for the Philippines)*. 2016.
Note 8) The World Bank. *Global Solar Atlas 2.0, Solar Resource Data: Solargis*. Washington DC, 2021.
Note 9) Ember. Progress towards Clean Power Targets The Philippines 2000–2040. *Yearly Electricity Data*. https://ember-climate.org/countries-and-regions/countries/philippines-the/.
Note 10) NREL. *Life Cycle Greenhouse Gas Emissions from Solar Photovoltaics*. Golden, CO, 2012.

REFERENCES

1) Garabitos Lara E, Santos García F. Review on viability and implementation of residential PV-battery systems: Considering the case of Dominican Republic. *Energy Reports*. 2021;7:8868-8899. doi:10.1016/j.egyr.2021.11.208
2) Hyun S, Taghizadeh-Hesary F, Shim HS. Modeling solar energy system demand using household-level data in Myanmar. *Econ Anal Policy*. 2021;69:629-639. doi:10.1016/j.eap.2021.01.011

3) Nazari-Heris M, Asadi S. Reliable energy management of residential buildings with hybrid energy systems. *Journal of Building Engineering*. 2023;71. doi:10.1016/j.jobe.2023.106531
4) Panicker K, Anand P, George A. Assessment of building energy performance integrated with solar PV: Towards a net zero energy residential campus in India. *Energy Build*. 2023;281. doi:10.1016/j.enbuild.2022.112736
5) Vergel KBN, Marcelo KRS, Salison AJP, et al. Estimation of transportation energy demand of the Philippines using a bottom-up approach. *Asian Transport Studies*. 2022;8(January):100058. doi:10.1016/j.eastsj.2022.100058
6) Fu M, Kelly JA, Clinch JP. Estimating annual average daily traffic and transport emissions for a national road network: A bottom-up methodology for both nationally-aggregated and spatially-disaggregated results. *J Transp Geogr*. 2017;58:186-195. doi:10.1016/j.jtrangeo.2016.12.002
7) Sun D, Xia J. Research on road transport planning aiming at near zero carbon emissions: Taking Ruicheng County as an example. *Energy*. 2023;263(PB):125834. doi:10.1016/j.energy.2022.125834
8) García-Vázquez CA, Espinoza-Ortega H, Llorens-Iborra F, Fernández-Ramírez LM. Feasibility analysis of a hybrid renewable energy system with vehicle-to-home operations for a house in off-grid and grid-connected applications. *Sustain Cities Soc*. 2022;86. doi:10.1016/j.scs.2022.104124
9) Aguilar-Dominguez D, Dunbar A, Brown S. The electricity demand of an EV providing power via vehicle-to-home and its potential impact on the grid with different electricity price tariffs. *Energy Reports*. 2020;6:132-141. doi:10.1016/j.egyr.2020.03.007
10) Chen J, Zhang Y, Li X, et al. Strategic integration of vehicle-to-home system with home distributed photovoltaic power generation in Shanghai. *Appl Energy*. 2020;263. doi:10.1016/j.apenergy.2020.114603
11) Nishanthy J, Charles Raja S, Jeslin Drusila Nesamalar J. Feasibility analysis of solar PV system in presence of EV charging with transactive energy management for a community-based residential system. *Energy Convers Manag*. 2023;288. doi:10.1016/j.enconman.2023.117125
12) Andersen FM, Jacobsen HK, Gunkel PA. Hourly charging profiles for electric vehicles and their effect on the aggregated consumption profile in Denmark. *International Journal of Electrical Power and Energy Systems*. 2021;130(February). doi:10.1016/j.ijepes.2021.106900
13) Mitrakoudis SG, Alexiadis MC. Modelling Electric Vehicle Charge Demand : Implementation for the Greek Power System. *World Electr Veh J*. 2022;13(115). doi:https://doi.org/10.3390/ wevj13070115
14) Borge-Diez D, Icaza D, Açıkkalp E, Amaris H. Combined vehicle to building (V2B) and vehicle to home (V2H) strategy to increase electric vehicle market share. *Energy*. 2021;237:121608. doi:10.1016/J.ENERGY.2021.121608
15) Liu C, Chau KT, Wu D, Gao S. Opportunities and challenges of vehicle-to-home, vehicle-to-vehicle, and vehicle-to-grid technologies. *Proceedings of the IEEE*. 2013;101(11):2409-2427. doi:10.1109/JPROC.2013.2271951
16) Higashitani T, Ikegami T, Uemichi A, Akisawa A. Evaluation of residential power supply by photovoltaics and electric vehicles. *Renew Energy*. 2021;178:745-756. doi:10.1016/J.RENENE.2021.06.097
17) Zafar B, Abdullah S, Slama B. PV-EV integrated home energy management using vehicle-to-home (V2H) technology and household occupant behaviors. *Energy Strategy Reviews*. 2022;44(September):101001. doi:10.1016/j.esr.2022.101001
18) Kawasaki N, Muromachi Y. ACHIEVING ZERO-EMISSION CITY UTILIZING PV, EV AND BATTERY WITH CHARGING AND DISCHARGING CONTROL. *Journal of Japan Society of Civil Engineers, Ser D3 (Infrastructure Planning and Management)*. 2022;77(5):29-38.
19) Japan International Cooperation Agency (JICA), Department of Transportation and Communications (DOTC), ALMEC Corporation, Oriental Consultants Global Co. Ltd. *MMUTIS Update and Enhancement Project (MUCEP)*.; 2015.
20) Abaya EB, Vergel KB, Quiros EN, Sigua R. Development of Drive Cycles and Measurement of Fuel Economies of Light Duty Vehicles in Metro Manila. *SAE Technical Papers*. 2018;2018-Septe:1-11. doi:10.4271/2018-01-1758
21) Goswami DY. *Principles of Solar Engineering*. Third. CRC PRess; 2015.
22) Martinez-Gracia A, Arauzo I, Uche J. Solar energy availability. In: *Solar Hydrogen Production: Processes, Systems and Technologies*. Academic Press; 2019:113-149. doi:10.1016/B978-0-12-814853-2.00005-9
23) Erbs DG, Klein SA, Duffle JA. Estimation of the diffuse radiation fraction for hourly, daily and monthly-average global radiation. *Solar Energy* . 1982;28(4):293-302.
24) Perez R, Ineichen P, Seals R, Michalsky J, Stewart R. Modeling daylight availability and irradiance components from direct and global irradiance. *Solar Energy*. 1990;44(5):271-289. doi:10.1016/0038-092X(90)90055-H
25) Kirillov A, Mintun E, Ravi N, et al. Segment Anything. *arXiv:230402643*. Published online April 5, 2023.
26) Wu Q, Osco L. samgeo: A Python package for segmenting geospatial data with the Segment Anything Model (SAM). *Zenodo*. Published online 2023. doi:10.5281/zenodo.7966658
27) Basaraner M, Cetinkaya S. Performance of shape indices and classification schemes for characterising perceptual shape complexity of building footprints in GIS. *International Journal of Geographical Information Science*. 2017;31(10):1952-1977. doi:10.1080/13658816.2017.1346257
28) García-Vázquez CA, Espinoza-Ortega H, Llorens-Iborra F, Fernández-Ramírez LM. Feasibility analysis of a hybrid renewable energy system with vehicle-to-home operations for a house in off-grid and grid-connected applications. *Sustain Cities Soc*. 2022;86(July). doi:10.1016/j.scs.2022.104124
29) Zhong T, Zhang Z, Chen M, et al. A city-scale estimation of rooftop solar photovoltaic potential based on deep learning. *Appl Energy*. 2021;298. doi:10.1016/j.apenergy.2021.117132